iScience

CellPress

Perspective

Important Considerations in Plasmon-Enhanced Electrochemical Conversion at Voltage-Biased Electrodes

Elizabeth R. Corson,[1,2,6] Erin B. Creel,[1,3,4,6,7] Robert Kostecki,[1,5] Bryan D. McCloskey,[1,2,5] and Jeffrey J. Urban[1,3,*]

In this perspective we compare plasmon-enhanced electrochemical conversion (PEEC) with photoelectrochemistry (PEC). PEEC is the oxidation or reduction of a reactant at the illuminated surface of a plasmonic metal (or other conductive material) while a potential bias is applied. PEC uses solar light to generate photoexcited electron-hole pairs to drive an electrochemical reaction at a biased or unbiased semiconductor photoelectrode. The mechanism of photoexcitation of charge carriers is different between PEEC and PEC. Here we explore how this difference affects the response of PEEC and PEC systems to changes in light, temperature, and surface morphology of the photoelectrode.

INTRODUCTION

Plasmon-enhanced electrochemical conversion (PEEC) is performed by illuminating the surface of a plasmonic electrode while applying a potential to reduce or oxidize a reactant (Figure 1B). This underexplored field presents new opportunities for sustainable production of fuels and value-added chemicals. PEEC is related to the established field of photoelectrochemistry (PEC) where solar light is converted to electron-hole pairs at a biased or unbiased semiconductor photoelectrode to drive an electrochemical reaction, typically water splitting (Figure 1A). In this perspective we compare PEEC with PEC and discuss how standards developed in the field of PEC regarding temperature control, light flux measurement, and electrode stability characterization relate to the study of PEEC.

The origins of PEC and PEEC can be traced to the discovery of the photoelectric effect by Becquerel (1839), with pioneering advancements made on illuminated metal electrodes by Gerischer and Delahay (1961). The first reported PEC reaction was water splitting at an illuminated TiO_2 anode (Boddy, 1968; Fujishima and Honda, 1972). PEC water splitting has been extensively explored and reviewed (Bak et al., 2002; Grätzel, 2001; Kudo and Miseki, 2009) and, to a lesser extent, other PEC reactions such as carbon dioxide (CO_2) reduction (Ganesh, 2011; Kumar et al., 2012; Zhao et al., 2014) and oxidation of organics (Georgieva et al., 2012; Lianos, 2011). The first report of PEEC was the extraction of plasmonically excited hot electrons and holes at a silver electrode (Sass et al., 1974). Despite the comparable age, PEEC has been the subject of many fewer studies than PEC. Reported PEEC reactions include CO_2 reduction (Creel et al., 2019; Kostecki and Augustynski, 1994), oxygen (O_2) reduction (Shi et al., 2019; Zheng et al., 2017), and hydrogen (H_2) evolution (Guo et al., 2018; Wilson et al., 2019; Zhang et al., 2018).

A schematic comparing the different mechanisms of photoexcitation of charge carriers for PEC and PEEC is shown in Figure 1. The goal in PEC is to completely drive the reaction with sunlight, although an external potential bias is often needed to overcome the reaction activation barrier. In most semiconductor-driven PEC, there is little to no electrochemical activity observed under dark conditions. In contrast, the aim in PEEC is to couple illumination with an applied voltage to influence the catalyst selectivity and activity. In other words, there will be electrochemical activity without illumination in PEEC, and it is important to compare illuminated ("light") and unilluminated ("dark") performance to discern the impact of the light. In PEEC the total photocurrent can be distinguished from overall activity (often by chopped light experiments), but it can be difficult to precisely quantify how individual product formation changes upon illumination if products are formed in the dark and the light. The dark current may be quite high compared with the photocurrent, which can make it challenging to detect subtle changes in product selectivity that are driven by the light. This need in PEEC to precisely compare dark and light performance motivates the essential use of temperature control.

TEMPERATURE CONTROL

In PEC, temperature control is recommended (Chen et al., 2013) to ensure that experiments performed at room temperature are comparable between labs. PEC cells must be designed to withstand heating from a

[1]Joint Center for Artificial Photosynthesis, Lawrence Berkeley National Laboratory, Berkeley, CA 94720, USA

[2]Department of Chemical and Biomolecular Engineering, University of California, Berkeley, CA 94720, USA

[3]The Molecular Foundry, Lawrence Berkeley National Laboratory, Berkeley, CA 94720, USA

[4]Department of Chemistry, University of California, Berkeley, CA 94720, USA

[5]Energy Storage and Distributed Resources Division, Lawrence Berkeley National Laboratory, Berkeley, CA 94720, USA

[6]These authors contributed equally

[7]Present address: Oak Ridge National Laboratory, Oak Ridge, TN 37830, USA

*Correspondence: jjurban@lbl.gov

https://doi.org/10.1016/j.isci.2020.100911

This is an open access article under the CC BY-NC-ND license (http://creativecommons.org/licenses/by-nc-nd/4.0/).

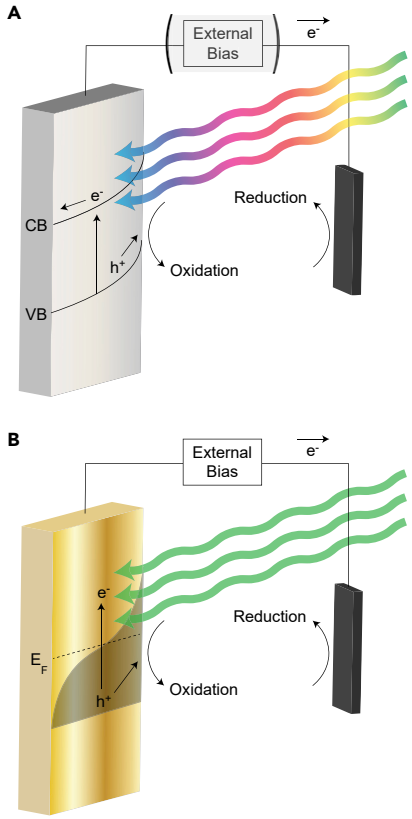

Figure 1. Comparison of the Mechanism of Photoexcitation of Charge Carriers in PEC and PEEC

(A) In this PEC example the photoanode is an n-type semiconductor illuminated by solar light. When the energy of light exceeds the band gap, photoexcited electrons move from the valence band (VB) to the conduction band (CB) and through the external circuit to the cathode to drive the reduction reaction. Holes remaining in the VB propel the oxidation reaction. An external bias is optional in PEC.

(B) In this PEEC example the photoanode is a plasmonic metal illuminated by a single wavelength of light matching the plasmonic resonance. The photoexcited electrons move from filled electronic states to higher energy unfilled states, resulting in an electron distribution with a higher population above the Fermi level (E_F). The holes with sufficient energy promote the oxidation reaction. An external bias is always applied in PEEC, in this case to tune the E_F of the plasmonic anode and provide electrons for the reduction reaction at the cathode.

100 mW cm^{-2} solar light source. In contrast, PEEC cells are often exposed to higher intensity light sources at a single wavelength to maximize photocurrent. This difference is highlighted in Figure 1. Light absorption of water is low at UV and visible wavelengths and highest at infrared (IR) wavelengths (Döscher et al., 2014; Xiang et al., 2019). IR wavelengths are present in solar light used in PEC, whereas PEEC studies typically use light in the UV and visible wavelength ranges, so one might expect less cell heating in PEEC. However, light absorption of water can vary with ion concentration. Commonly used electrolyte salts such as potassium bicarbonate ($KHCO_3$) and sulfuric acid (H_2SO_4) absorb strongly in the near-UV, as shown in Figure 3B. In addition, cell heating can be caused by light absorption of the cell components and electrode, not just the electrolyte.

As shown in Figure 2A, continuous illumination of a PEEC cell by a single wavelength LED can lead to dramatic heating of the system. The unregulated temperature of the electrolyte in this cell (Corson et al., 2018), which was designed with a low electrolyte volume to increase detectability of liquid products, rose by 12 K in 20 min—and would have continued to rise had the experiment not been terminated—under constant illumination by a 170 mW cm^{-2} 365 nm light-emitting diode (LED). This temperature rise demonstrates that PEEC cells are susceptible to heating whether the light source is a broadband incandescent bulb or a monochromatic beam.

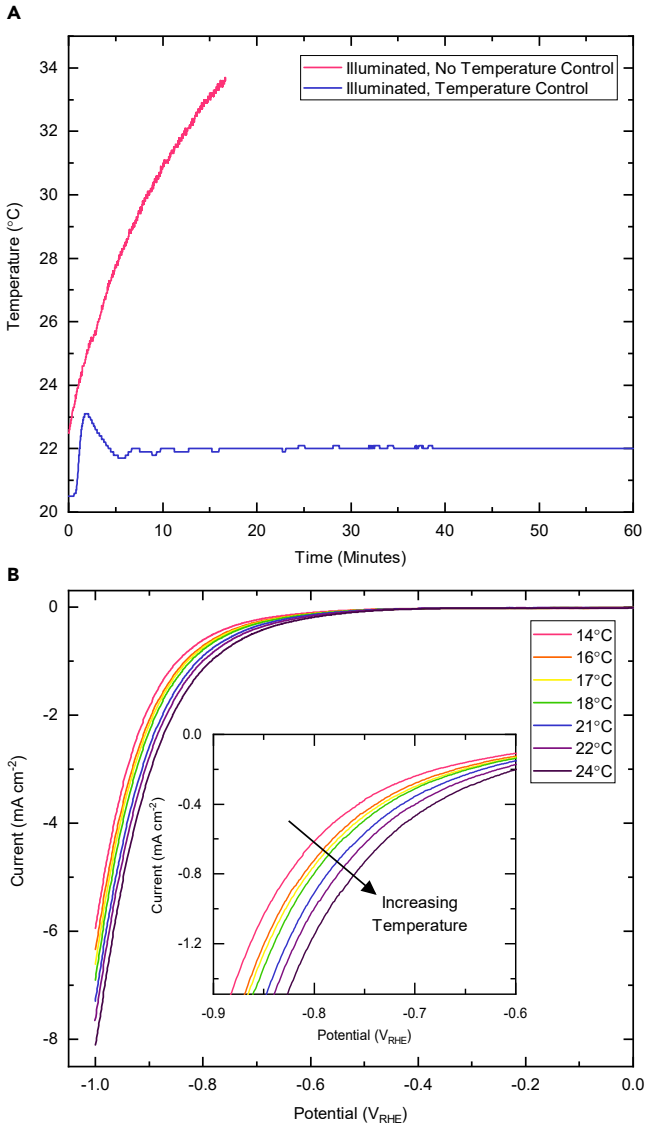

Figure 2. Temperature Rise with Single-Wavelength Illumination and the Effect of Heating on the Total Current

(A) Electrolyte temperature in a low-volume PEEC cell (Corson et al., 2018) over time with and without temperature control when illuminated with a 365 nm 2.5 W LED.

(B) Linear sweep voltammetry at 100 mV s^{-1} at a plasmonic silver cathode in CO_2-saturated 0.5 M potassium carbonate (K_2CO_3) electrolyte at various electrolyte temperatures. CO_2 flows continuously through the cell at 5 sccm. Inset is the same data in a smaller potential range to demonstrate activity increase with increasing temperature.

In any catalytic system the Arrhenius equation predicts that reaction rate constants depend exponentially on temperature. As current is directly related to the reaction rate, one expects the current to increase with increasing temperature. However, there are multiple phenomena in PEC and PEEC beyond reaction kinetics that also depend on temperature and can influence the current density and product distribution.

A consideration that only affects PEC is the semiconductor bandgap, which may decrease with increasing temperature causing the photovoltage to decrease (Haussener et al., 2013). This decrease in the photovoltage may counteract the reaction rate increase, suppressing the overall increase in current density at a higher temperature. In contrast, for PEEC the rate of hot carrier generation is expected to increase with temperature due to the increase in phonon-assisted electronic transitions (Brown et al., 2016), which would contribute to an increase in the photocurrent density.

Another reason for the importance of temperature regulation in PEC and PEEC is that increasing the electrolyte temperature typically causes the solubility of gases to decrease exponentially, as described by the van't Hoff equation. This can greatly decrease the reactant concentration for both PEC and PEEC systems where the reactant is a gas, as in CO_2 reduction or nitrogen (N_2) reduction, which may affect the product distribution. In addition, as each elementary reaction has a different temperature dependence according to their respective activation energies and pre-exponential factors, increasing the temperature may change the product distribution (Corson et al., 2018).

An example of how the current is affected by changes in temperature can be seen in Figure 2B where linear sweep voltammetry is performed at a plasmonic silver cathode where CO_2 reduction and H_2 evolution are occurring. The magnitude of the current density increases when the electrolyte temperature is increased by just 1 or 2 K from 14°C to 24°C. At −1.0 V versus the reversible hydrogen electrode (V_{RHE}) there is a 30% difference between the highest and lowest current densities across this modest 10 K temperature range, a range we have shown can easily be exceeded in an illuminated cell when the temperature is not controlled (Figure 2A). Similarly, Guo et al. (2018) showed that the current density at plasmonic Pt/Fe-Au nanorods during PEEC H_2 evolution increased by 33% when the temperature was raised from 20 to 30°C at −0.05 V_{RHE} while illuminated by an 808 nm laser. In comparison, Dias et al., 2016 reported that the photocurrent density at a WO_3 photoanode for PEC water splitting increased by 5% when the temperature was increased from 25 to 35°C at 1.7 V_{RHE}. This difference in the magnitude of the current density increase with a 10 K temperature rise between a PEC and PEEC system may reflect the opposing phenomena of bandgap decrease in PEC and increase in the rate of hot carrier generation in PEEC. When compared with PEC, the potentially greater impact of temperature makes it imperative in PEEC to use a temperature-controlled cell with precision of at least 1 K, especially when comparing light and dark activity and product distributions.

Effective cell temperature control requires incorporation of a temperature probe in contact with the electrolyte, ideally as close to the working electrode as possible, a cooling method, and a proportional-integral-derivative (PID) controller. The selection and sizing of the cooling method depends on the cell geometry and the maximum light intensity desired, as this will define the maximum heat removal needs of the system. Although complete cell submersion in a water bath would make light incorporation difficult, a circulating bath connected to a cooling jacket or integrated heat-transfer channels within the cell can be designed to allow electrode illumination (Zavarine and Kubiak, 2001). Another possible cooling system is a solid-state Peltier element with a heat sink and fan (Corson et al., 2018).

LIGHT FLUX AT THE ELECTRODE

An important figure of merit in PEC water splitting is the solar-to-hydrogen (STH) efficiency. Although STH is not relevant for PEEC studies that use a non-solar light source or investigate reactions other than H_2 evolution, there are efficiency standards from the field of PEC that can be used in PEEC. The most applicable are the two ways to measure the quantum efficiency of light utilization for a given electrode: external quantum efficiency (EQE) and internal quantum efficiency (IQE) (Chen et al., 2010).

$$\mathrm{EQE} = \frac{\text{photogenerated electrons/s}}{\text{incident photons/s}} \qquad \text{(Equation 1a)}$$

$$\mathrm{IQE} = \frac{\text{photogenerated electrons/s}}{\text{absorbed photons/s}} \qquad \text{(Equation 1b)}$$

EQE is the ratio of photogenerated electrons to *incident* photons. In PEC, typical EQE values are greater than 10% and can approach 100% for wavelengths above the bandgap (Shi et al., 2015). In contrast, PEEC systems without semiconductor or molecular co-absorbers typically have EQE values below 1% at the plasmon resonance wavelength (Kim et al., 2018; Robatjazi et al., 2015). For example, if we compare PEC with PEEC for CO_2 reduction at −0.9 V_{RHE} in neutral electrolyte under 360 nm illumination, a ZnTe photocathode has an EQE of 80% (Jang et al., 2014), whereas a plasmonic silver cathode has an EQE of 0.45% (Kim et al., 2018).

IQE is the ratio of photogenerated electrons to *absorbed* photons. IQE is generally higher than EQE for both PEC and PEEC materials due to the exclusion of losses from photons that are transmitted or reflected. However, the difference in order of magnitude between PEC and PEEC electrodes found in EQE still exists for IQE. From the previous CO_2 reduction example, the semiconductor IQE is 100% (Jang et al., 2014), whereas the plasmonic metal IQE is 1.2% (Kim et al., 2018).

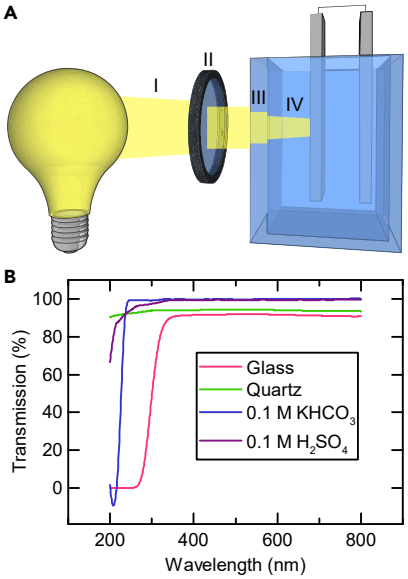

Figure 3. Light Intensity Attenuation from the Light Source to the Plasmonic Electrode Surface

(A) Light intensity per unit area decreases (I) as a function of distance from a non-collimated source, (II) when passing through optical lenses or filters, (III) when passing through electrochemical cell walls, and (IV) when passing through electrolyte.

(B) Transmission spectra of a 1-mm-thick glass slide, 2-mm-thick quartz window, 1 cm path length through 0.1 M $KHCO_3$, and 1 cm path length of 0.1 M H_2SO_4. Transmission spectra of glass and quartz are measured relative to air. Transmission spectra of salt solutions are measured in a quartz cuvette relative to a quartz cuvette filled with ultrapure water.

One key difference for the disparity in PEC and PEEC efficiencies is carrier lifetime. Photoexcited electrons and holes in semiconductors can have lifetimes on the order of nanoseconds (Abdi et al., 2013), whereas excited carriers in plasmonic metals exist for less than a picosecond (Boerigter et al., 2016) due to the high density of electronic states in metals and other conductive media (Figure 1). Due to their brief existence, plasmonically generated excited carriers must be co-located with the charge-accepting species in order for charge transfer to occur. In contrast, photoexcited carriers in semiconducting materials have time to diffuse to the solid-liquid interface and can have diffusion lengths on the order of tens of nanometers (Abdi et al., 2013). These differences in carrier lifetime and diffusion length help explain why the EQE and IQE values of plasmonic metals used in PEEC are much lower than that of semiconducting materials used in PEC.

Just as in PEC, reporting the EQE and IQE in PEEC will deconvolute a material's ability to separate and collect photoexcited electrons and holes from its optical absorption. This provides insight for further optimization of the material's optical absorption or extraction of charge carriers.

Calculating EQE and IQE requires measuring the incident light intensity. It is important to measure the light *at the electrode surface*, especially in studies that focus on catalyst performance and mechanism rather than overall device efficiency. Glass, quartz, water, common electrolytes, and gas bubbles can all have significant reflection or absorption, making the light intensity incident on the photoelectrode significantly less than the light intensity incident on the cell (Figure 3). For example, Figure 3 shows that the transmission of light through glass is reduced by 50% at a wavelength of 350 nm and is completely blocked for wavelengths below 300 nm. This means that if the light intensity were measured before the light passed through the glass, the reported EQE and IQE values for the photoelectrode would be half of the actual values at 350 nm.

Researchers should also bear in mind that the optical properties of all materials are temperature dependent (Xiang et al., 2019). Although full device research, common in PEC, incorporates short path lengths through electrolyte and anti-reflective coatings on cell windows (Xiang et al., 2019), most laboratory-scale PEEC cells are not designed with maximum light transmission to the plasmonic electrode in mind. Thus, the light attenuation may be significant. Low light intensity may impact the signal-to-noise ratio between the photocurrent and background "dark" current as plasmonic photoactivity increases with light intensity. Additionally, it may be difficult to control the temperature of electrochemical cells that are not designed for high light transmission due to the high light intensity needed to achieve a measurable photocurrent.

The light attenuation through the electrochemical cell walls and electrolyte becomes especially important with broad-spectrum illumination because the light transmission of cell components is wavelength dependent and often has especially low transmission in the UV or IR regions of the spectrum (Figure 3B). Although

glass is often replaced with quartz for UV transmission, the effect of the absorption of water (Döscher et al., 2014) or the electrolyte salt is not commonly accounted for.

Additionally, both PEC and PEEC researchers should confirm that the cell components intended to define the illumination and active area of a photoelectrode (e.g., epoxy or o-rings) are opaque for all of the light spectrum (not just the visible) that will be used for illumination. A UV-transmissive epoxy or o-ring, for example, could result in the photoactive area of an electrode being much larger than the electrochemically active area (Döscher et al., 2014). For example, in a cell with an electrochemically active area of 1.0 cm^2 and an o-ring outer diameter (OD) of 1.4 cm, a UV-transmissive o-ring would result in an actual illumination area of 1.6 cm^2, an increase of 60%.

Light power incident on the cell can be measured with a power meter, thermopile, or photodiode and then corrected to find the light power incident on the plasmonic electrode using the transmission of the cell components. For broad-spectrum illumination most common in PEC, it is important to measure the light spectrum rather than just the light intensity because of the wavelength dependence of the photoactivity (Tian and Tatsuma, 2004) and the wavelength dependence of the optical properties of the cell components. The method for correcting spectral mismatch between a lamp and solar irradiance (Döscher et al., 2014) is also suitable for correcting for decreased transmission of cell components.

Standards for calibrating light sources to closely match the AM 1.5 G spectrum have been well defined within the field of PEC (Chen et al., 2013; Döscher et al., 2016; van de Krol and Grätzel, 2012; May et al., 2017). Although these standards can be directly applied to PEEC systems for broad-spectrum illumination studies, they are not relevant for single-wavelength light experiments that are commonly used in the field of PEEC. High-intensity single-wavelength illumination at the plasmon resonance wavelength can help increase the photocurrent for PEEC systems, improving the signal-to-noise ratio and enhancing the difference in product distribution between light and dark conditions. Varying the light intensity at a single wavelength is also prevalent in PEEC studies. A linear relationship between photocurrent and light intensity demonstrates that the mechanism is photonic, as a thermal process would result in an exponential relationship (Kale et al., 2014). Probing behavior at different wavelengths can lead to a fundamental understanding of the mechanism of plasmon-enhanced charge transfer (Boerigter et al., 2016). To accurately compare different PEEC electrodes it is important that researchers measure and report the light spectrum and intensity at the electrode surface for any illuminated experiments.

SURFACE CHANGES UNDER REACTION CONDITIONS

The activity and performance of all photoelectrocatalysts depend on the specific surface morphologies and structural features (e.g., high index planes, step edges). Both PEC and PEEC photoelectrode behavior can be extremely sensitive to nanoscale morphology. In PEC, nanofeatures can influence charge separation and transport, scattering rate, and the size of the band gap (Shen et al., 2018). For example, Wu et al. (2013) showed that increasing the length of silicon nanowires by 700 nm decreased the photocurrent by 40% at 1.0 V, whereas the minority carrier lifetime decreased by just 2% during PEC bromide reduction. They related these effects to changes in light adsorption and photogenerated carrier collection caused by the increased length. In PEEC, the size, shape, and proximity of nanostructures can change the peak plasmon resonance wavelength, energy distribution and number of hot carriers, and intensity of the local electric field (Linic et al., 2011; Link and El-Sayed, 2000; Manjavacas et al., 2014; Shi et al., 2019 demonstrated that changing from silver nanowires to nanotriangles caused the plasmon resonance to red-shift by 50%, the maximum electric field enhancement to triple, and the photocurrent to increase by 33% at 0.65 V_{RHE} during O_2 reduction. These changes were attributed to enhanced light adsorption and a higher rate of hot electron production. It is clear that changes to the surface morphology of PEC and PEEC photoelectrodes on the scale of nanometers can significantly impact their performance, but the underlying physical reason for this change is inherently different between the two fields due to the distinct mechanisms of photoexcitation of charge carriers. Therefore, changes in nanofeatures that benefit one system may be detrimental to the other.

Active catalysts can delaminate from the electrode surface or undergo dramatic morphological, composition, phase, and activity changes under reaction conditions (Hodnik et al., 2016; Tao and Salmeron, 2011) or when exposed to voltage (Creel et al., 2019). All of these changes can impact not only the catalytic performance but also the optical properties of the PEC or PEEC photoelectrode. Thus, it is critical to characterize

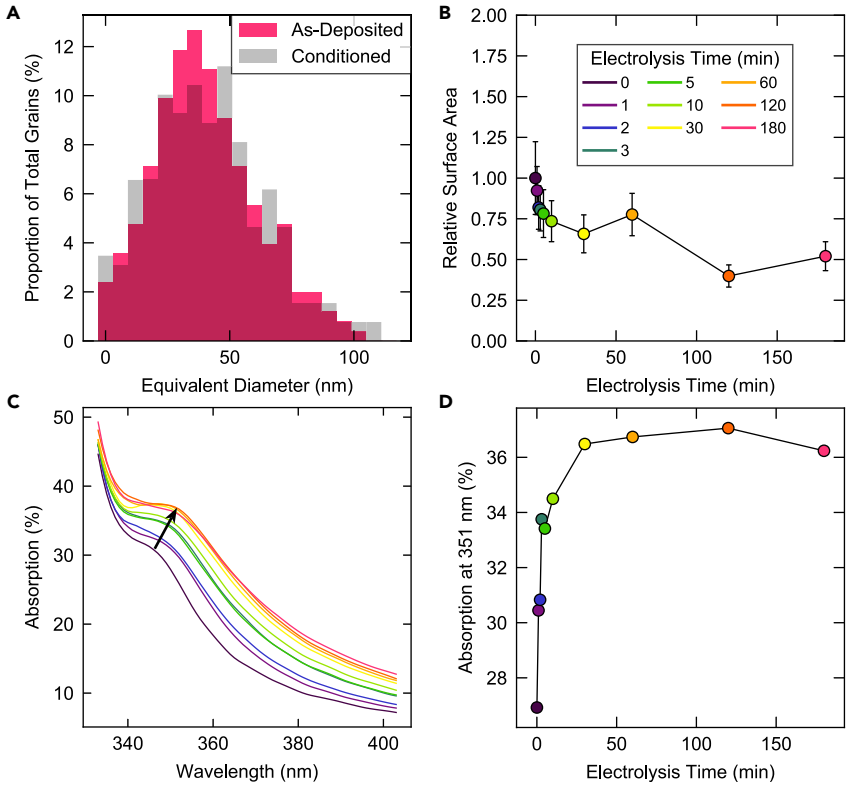

Figure 4. Changes in Morphology and Optical Properties of a Silver Thin Film Cathode after CO_2 Electrolysis without Illumination in 0.5 M K_2CO_3 at −1.1 V_{RHE}

The electrode was made by electron beam (e-beam) depositing 200 nm of silver over a glass slide with 5 nm of titanium used as an adhesion layer.

(A) Comparison of the silver grain size distribution on the cathode in terms of equivalent diameter—the diameter of a circle with the same projected area as the projected area of the grain—as measured by AFM. "As-Deposited" indicates a silver film that has not been used as an electrode, and "Conditioned" indicates that the silver thin film has undergone 45 min of CO_2 electrolysis.

(B) Evolution of the ECSA of the cathode relative to the as-deposited silver film after various CO_2 electrolysis times. Legend for parts B–D where electrolysis time is the time that the silver electrode was used as a CO_2 electrolysis cathode. Error bars represent one standard deviation.

(C) Evolution of the UV-visible absorption spectra of the cathode after various CO_2 electrolysis times.

(D) Evolution of the absorption of the electrode at 351 nm after various CO_2 electrolysis times. Absorption is calculated as 100% − %R where %R is the total reflection measured by an integrating sphere. Figures adapted from Creel et al. (2019).

microscopic catalyst evolution and any differences in optical properties in order to understand and control or prevent morphological changes induced by reaction conditions.

Researchers often use the stability of the current over time in long-term constant voltage experiments as a measure of electrode stability, but this method gives no insight into the mechanism for activity degradation. It is well known that successive oxidation and reduction cycles can degrade catalysts, but constant-voltage experiments also induce catalyst dissolution, corrosion, and restructuring. Our recent PEEC study of a plasmonic silver thin film cathode showed decreased electrochemical surface area (ECSA), increased broad-spectrum absorption, and a broader grain size distribution after performing CO_2 electrolysis without illumination (Figure 4). We found that the changes in optical properties and electrochemical surface area changed quickly in the first few minutes of applied potential but reached a steady state between 30 and 60 min of electrolysis. In this case, we were able to "electrochemically condition" the plasmonic silver cathode for 45 min to achieve stable performance over hours. After 45 min the absorption at the plasmon resonance was 37% higher and the relative surface area was 50% lower than the as-prepared electrode (Creel et al., 2019).

	PEC	PEEC
Experimental		
Photoelectrode	Semiconductor	Metal or other conductive material
Mechanism	Band gap excitation	Plasmon excitation
Applied Potential	Optional	Always
Temperature Increase		
Reaction Kinetics	↑ Reaction rate constants	↑ Reaction rate constants
Solubility	↓ Gaseous reactants	↓ Gaseous reactants
Electron Excitation	↓ Photovoltage	↑ Hot carrier generation rate
Light Flux		
Efficiency	IQE and EQE >10%	IQE and EQE <1%
Typical Light Source	Broadband	Monochromatic
Surface Morphology		
Nanoscale Changes	Can impact charge carrier dynamics and band edge positions	Can impact plasmon resonance wavelength, hot carrier distribution, and local electric field intensity

Table 1. Comparison of PEC and PEEC

An analogous example from PEC is the anodic photocorrosion of GaN (Sato et al., 2009). The researchers observed that the photocurrent decreased over time during H_2 evolution in aqueous 1.0 M NaOH. A surface morphology study by AFM revealed that the root-mean-square (RMS) roughness continued to increase throughout the 22-h photoelectrochemical experiment. In contrast to the previous PEEC example, this electrochemically induced surface morphology change never stabilized and was detrimental to the photoelectrode performance.

Measuring the changes in morphology during any electrochemical reaction is critical when attempting to understand the structure-function relationships of an electrode. It is especially important for PEEC researchers to check for reaction-induced morphology changes because small structural changes may modify the optical properties of the plasmonic electrode significantly (Figure 4) (Linic et al., 2011; Link and El-Sayed, 2000; Manjavacas et al., 2014). Changes to the absorption of the electrode will alter the IQE as well as the photoactivity. Both PEC and PEEC researchers should, at a minimum, compare the morphology and optical changes before and after PEC using scanning electron microscopy (SEM), transmission electron microscopy (TEM), atomic force microscopy (AFM), UV-visible spectroscopy, or other readily available techniques (Chen et al., 2013).

CONCLUSION

We have shown that standards developed in the established field of PEC can be used to build best practices for PEEC. The key distinctions and similarities between PEC and PEEC presented in this perspective are summarized in Table 1. Cell temperature control is still critical for PEEC, especially when comparing light and dark performance. Although not all efficiency measures from PEC are relevant to PEEC, EQE and IQE are valid and useful for characterizing plasmonic electrodes. However, it is important to recognize that fundamental differences between semiconductors and plasmonic metals result in EQE and IQE values for PEEC systems that are often two orders of magnitude lower than PEC systems. Surface morphology can affect the catalytic and optical properties of semiconductors and plasmonic metals. Changes to the surface induced by reaction conditions should be monitored and controlled for repeatable results. By learning from the 50-year history of PEC water splitting we can ensure that PEEC research is comparable and reproducible.

ACKNOWLEDGMENTS

This work was largely supported by the National Science Foundation under Grant No. CBET-1653430. This material is based upon work performed by the Joint Center for Artificial Photosynthesis, a DOE Energy

Innovation Hub, supported through the Office of Science of the U.S. Department of Energy under Award No. DE-SC0004993. Work at the Molecular Foundry was supported by the Office of Science, Office of Basic Energy Sciences of the U.S. Department of Energy under Contract No. DE-AC02-05CH11231. E.R.C. and E.B.C. acknowledge support from the National Science Foundation Graduate Research Fellowship under Grant No. DGE 1106400.

AUTHOR CONTRIBUTIONS

Conceptualization, E.R.C., E.B.C., and J.J.U.; Investigation, E.R.C. and E.B.C.; Writing—Original Draft, E.R.C. and E.B.C.; Writing—Review & Editing, E.R.C., E.B.C., R.K., B.D.M., and J.J.U.; Funding Acquisition, R.K., B.D.M., and J.J.U.

REFERENCES

Abdi, F.F., Savenije, T.J., May, M.M., Dam, B., and van de Krol, R. (2013). The origin of slow carrier transport in $BiVO_4$ thin film photoanodes: a time-resolved microwave conductivity study. J. Phys. Chem. Lett. *4*, 2752–2757.

Bak, T., Nowotny, J., Rekas, M., and Sorrell, C. (2002). Photo-electrochemical hydrogen generation from water using solar energy. Materials-related aspects. Int. J. Hydrogen Energ. *27*, 991–1022.

Becquerel, E. (1839). Recherches sur les effets de la radiation chimique de la lumière solaire, au moyen des courants électriques. Compt. Rend. Acad. Sci. *9*, 145–149.

Boddy, P.J. (1968). Oxygen evolution on semiconducting TiO_2. J. Electrochem. Soc. *115*, 199–203.

Boerigter, C., Aslam, U., and Linic, S. (2016). Mechanism of charge transfer from plasmonic nanostructures to chemically attached materials. ACS Nano *10*, 6108–6115.

Brown, A.M., Sundararaman, R., Narang, P., Goddard, W.A., and Atwater, H.A. (2016). Nonradiative plasmon decay and hot carrier dynamics: effects of phonons, surfaces, and geometry. ACS Nano *10*, 957–966.

Chen, Z., Dinh, H.N., and Miller, E. (2013). Photoelectrochemical Water Splitting Standards, Experimental Methods, and Protocols (Springer).

Chen, Z., Jaramillo, T.F., Deutsch, T.G., Kleiman-Shwarsctein, A., Forman, A.J., Gaillard, N., Garland, R., Takanabe, K., Heske, C., Sunkara, M., et al. (2010). Accelerating materials development for photoelectrochemical hydrogen production: standards for methods, definitions, and reporting protocols. J. Mater. Res. *25*, 3–16.

Corson, E.R., Creel, E.B., Kim, Y., Urban, J.J., Kostecki, R., and McCloskey, B.D. (2018). A temperature-controlled photoelectrochemical cell for quantitative product analysis. Rev. Sci. Instrum. *89*, 055112.

Creel, E.B., Corson, E.R., Eichhorn, J., Kostecki, R., Urban, J.J., and McCloskey, B.D. (2019). Directing selectivity of electrochemical carbon dioxide reduction using plasmonics. ACS Energy Lett. *4*, 1098–1105.

Dias, P., Lopes, T., Meda, L., Andrade, L., and Mendes, A. (2016). Photoelectrochemical water splitting using WO_3 photoanodes: the substrate and temperature roles. Phys. Chem. Chem. Phys. *18*, 5232–5243.

Döscher, H., Geisz, J.F., Deutsch, T.G., and Turner, J.A. (2014). Sunlight absorption in water – efficiency and design implications for photoelectrochemical devices. Energy Environ. Sci. *7*, 2951–2956.

Döscher, H., Young, J.L., Geisz, J.F., Turner, J.A., and Deutsch, T.G. (2016). Solar-to-hydrogen efficiency: shining light on photoelectrochemical device performance. Energy Environ. Sci. *9*, 74–80.

Fujishima, A., and Honda, K. (1972). Electrochemical photolysis of water at a semiconductor electrode. Nature *238*, 37–38.

Ganesh, I. (2011). Conversion of carbon dioxide to methanol using solar energy - a brief review. Mater. Sci. Appl. *2*, 1407–1415.

Georgieva, J., Valova, E., Armyanov, S., Philippidis, N., Poulios, I., and Sotiropoulos, S. (2012). Bi-component semiconductor oxide photoanodes for the photoelectrocatalytic oxidation of organic solutes and vapours: a short review with emphasis to TiO_2–WO_3 photoanodes. J. Hazard. Mater. *211–212*, 30–46.

Gerischer, H., and Delahay, P. (1961). Advances in Electrochemistry and Electrochemical Engineering (Wiley).

Grätzel, M. (2001). Photoelectrochemical cells. Nature *414*, 338–344.

Guo, X., Li, X., Kou, S., Yang, X., Hu, X., Ling, D., and Yang, J. (2018). Plasmon-enhanced electrocatalytic hydrogen/oxygen evolution by Pt/Fe–Au nanorods. J. Mater. Chem. A *6*, 7364–7369.

Haussener, S., Hu, S., Xiang, C., Weber, A.Z., and Lewis, N.S. (2013). Simulations of the irradiation and temperature dependence of the efficiency of tandem photoelectrochemical water-splitting systems. Energy Environ. Sci. *6*, 3605–3618.

Hodnik, N., Dehm, G., and Mayrhofer, K.J.J. (2016). Importance and challenges of electrochemical in situ liquid cell electron microscopy for energy conversion research. Acc. Chem. Res. *49*, 2015–2022.

Jang, J.W., Cho, S., Magesh, G., Jang, Y.J., Kim, J.Y., Kim, W.Y., Seo, J.K., Kim, S., Lee, K.H., and Lee, J.S. (2014). Aqueous-solution route to zinc telluride films for application to CO_2 reduction. Angew. Chem. Int. Ed. *53*, 5852–5857.

Kale, M.J., Avanesian, T., and Christopher, P. (2014). Direct photocatalysis by plasmonic nanostructures. ACS Catal. *4*, 116–128.

Kim, Y., Creel, E.B., Corson, E.R., McCloskey, B.D., Urban, J.J., and Kostecki, R. (2018). Surface-plasmon-assisted photoelectrochemical reduction of CO_2 and NO_3^- on nanostructured silver electrodes. Adv. Energy Mater. *8*, 1800363.

Kostecki, R., and Augustynski, J. (1994). Electrochemical reduction of CO_2 at an activated silver electrode. Phys. Chem. *98*, 1510–1515.

van de Krol, R., and Grätzel, M. (2012). Photoelectrochemical Hydrogen Production (Springer).

Kudo, A., and Miseki, Y. (2009). Heterogeneous photocatalyst materials for water splitting. Chem. Soc. Rev. *38*, 253–278.

Kumar, B., Llorente, M., Froehlich, J., Dang, T., Sathrum, A., and Kubiak, C.P. (2012). Photochemical and photoelectrochemical reduction of CO_2. Annu. Rev. Phys. Chem. *63*, 541–569.

Lianos, P. (2011). Production of electricity and hydrogen by photocatalytic degradation of organic wastes in a photoelectrochemical cell: the concept of the photofuelcell: a review of a re-emerging research field. J. Hazard. Mater. *185*, 575–590.

Linic, S., Christopher, P., and Ingram, D.B. (2011). Plasmonic-metal nanostructures for efficient conversion of solar to chemical energy. Nat. Mater. *10*, 911–921.

Link, S., and El-Sayed, M.A. (2000). Shape and size dependence of radiative, non-radiative and photothermal properties of gold nanocrystals. Int. Rev. Phys. Chem. *19*, 409–453.

Manjavacas, A., Liu, J.G., Kulkarni, V.K., and Nordlander, P. (2014). Plasmon-induced hot carriers in metallic nanoparticles. ACS Nano *8*, 7630–7638.

May, M.M., Lackner, D., Ohlmann, J., Dimroth, F., van de Krol, R., Hannappel, T., and Schwarzburg, K. (2017). On the benchmarking of multi-junction photoelectrochemical fuel generating devices. Sustain. Energy Fuels *1*, 492–503.

Robatjazi, H., Bahauddin, S.M., Doiron, C., and Thomann, I. (2015). Direct plasmon-driven photoelectrocatalysis. Nano Lett. *15*, 6155–6161.

Sass, J.K., Sen, R.K., Meyer, E., and Gerischer, H. (1974). Effect of surface plasmon excitation on photoemission and photooxidation processes at a silver-electrolyte interface. Surf. Sci. *44*, 515–528.

Sato, K., Fujii, K., Koike, K., Goto, T., and Yao, T. (2009). Anomalous time variation of photocurrent in GaN during photoelectrochemical reaction for H_2 gas generation in NaOH aqueous solution. Phys. Status Solidi C *6*, S635–S638.

Shen, S., Chen, J., Wang, M., Sheng, X., Chen, X., Feng, X., and Mao, S.S. (2018). Titanium dioxide nanostructures for photoelectrochemical applications. Prog. Mater. Sci. *98*, 299–385.

Shi, F., He, J., Zhang, B., Peng, J., Ma, Y., Chen, W., Li, F., Qin, Y., Liu, Y., Shang, W., et al. (2019). Plasmonic-enhanced oxygen reduction reaction of silver/graphene electrocatalysts. Nano Lett. *19*, 1371–1378.

Shi, Z., Wen, X., Guan, Z., Cao, D., Luo, W., and Zou, Z. (2015). Recent progress in photoelectrochemical water splitting for solar hydrogen production. Ann. Phys. *358*, 236–247.

Tao, F., and Salmeron, M. (2011). In situ studies of chemistry and structure of materials. Science *331*, 171–174.

Tian, Y., and Tatsuma, T. (2004). Plasmon-induced photoelectrochemistry at metal nanoparticles supported on nanoporous TiO_2. Chem. Commun. (Camb.) *16*, 1810–1811.

Wilson, A.J., Mohan, V., and Jain, P.K. (2019). Mechanistic understanding of plasmon-enhanced electrochemistry. J. Phys. Chem. C *123*, 29360–29369.

Wu, S.L., Wen, L., Cheng, G.A., Zheng, R.T., and Wu, X.L. (2013). Surface morphology-dependent photoelectrochemical properties of one-dimensional Si nanostructure arrays prepared by chemical etching. ACS Appl. Mater. Interfaces *5*, 4769–4776.

Xiang, C., Walczak, K., Haber, J., Jones, R., Beeman, J.W., Guevarra, D., Karp, C., Liu, R., Shaner, M., Sun, K., et al. (2019). Prototyping development of integrated solar-driven water-splitting cells. In Integrated Solar Fuel Generators, I.D. Sharp, H.A. Atwater, and H.-J. Lewerenz, eds. (The Royal Society of Chemistry), pp. 387–453.

Zavarine, I.S., and Kubiak, C.P. (2001). A versatile variable temperature thin layer reflectance spectroelectrochemical cell. J. Electroanal. Chem. *495*, 106–109.

Zhang, H.X., Li, Y., Li, M.Y., Zhang, H., and Zhang, J. (2018). Boosting electrocatalytic hydrogen evolution by plasmon-driven hot-electron excitation. Nanoscale *10*, 2236–2241.

Zhao, J., Wang, X., Xu, Z., and Loo, J.S.C. (2014). Hybrid catalysts for photoelectrochemical reduction of carbon dioxide: a prospective review on semiconductor/metal complex co-catalyst systems. J. Mater. Chem. A *2*, 15228–15233.

Zheng, Z., Xie, W., Li, M., Ng, Y.H., Wang, D.-W., Dai, Y., Huang, B., and Amal, R. (2017). Platinum electrocatalysts with plasmonic nano-cores for photo-enhanced oxygen-reduction. Nano Energy *41*, 233–242.